

$\Gamma(K \rightarrow e\nu) / \Gamma(K \rightarrow \mu\nu)$ in the Minimal Supersymmetric Standard Model

Jennifer Girrbach^{1,2,3} and Ulrich Nierste¹

¹ *Institut für Theoretische Teilchenphysik, Karlsruhe Institute of Technology,
Universität Karlsruhe, Engesserstraße 7, 76128 Karlsruhe, Germany*

² *Institute of Advanced Study, Technische Universität München,
Lichtenbergerstraße 2a, 85748 Garching, Germany*

³ *Excellence Cluster Universe, Technische Universität München,
Boltzmannstraße 2, 85748 Garching, Germany*

Abstract

The quantity $R_K = \Gamma(K \rightarrow e\nu) / \Gamma(K \rightarrow \mu\nu)$ studied by the experiment NA62 at CERN is known to probe lepton-flavour violating (LFV) parameters of the Minimal Supersymmetric Standard Model (MSSM). A non-zero parameter δ_{RR}^{13} can open the decay channel $K \rightarrow e\nu_\tau$ and enhance R_K over its Standard-Model value. In the region of the parameter space probed by NA62 the contribution from a bino-stau loop diagram is numerically dominant and the mixing between left-handed and right-handed staus is important. For large values of the stau mixing angle θ_τ the commonly adopted mass insertion approximation is not accurate. We therefore express the supersymmetric contribution to R_K in terms of the mass of the lightest stau eigenstate, the mixing angle θ_τ , and other relevant MSSM parameter such as $\tan\beta$ and the charged-Higgs boson mass M_H and plot the parameter regions constrained by R_K . We further study to which extent R_K can be depleted through MSSM contributions interfering destructively with the SM amplitude for $K \rightarrow e\nu_e$. This lepton-flavour conserving (LFC) mechanism involves the parameter combination $|\delta_{LL}^{13} \delta_{RR}^{13}|$, which can be constrained with a naturalness consideration for the electron mass or with the measurement of the anomalous magnetic moment of the electron. The LFC effect on R_K is marginal, an NA62 measurement of R_K significantly below the Standard Model expectation would indicate physics beyond the MSSM.

1 Introduction

The discovery of neutrino oscillations has shown that individual lepton numbers are not conserved. This phenomenon constitutes physics beyond the Standard Model in its original formulation, which involves only renormalisable interactions and contains no right-handed neutrino fields. Nevertheless, the Standard Model can accommodate neutrino oscillations with the help of a dimension-5 term, which leads to a Majorana mass matrix for the neutrinos. By diagonalising this matrix one obtains the physical neutrino masses and the Pontecorvo-Maki-Nakagawa-Sakata (PMNS) matrix encoding the

strength of the flavour transitions [1, 2]. The dimension-5 mass term is naturally generated if right-handed neutrino fields are added to the Standard-Model (SM) Lagrangian: being gauge singlets these fields permit fundamental Majorana mass terms, which are not protected by the SM gauge symmetry and can consequently be very large. Integrating out the heavy right-handed neutrinos generates the dimension-5 term and the desired small neutrino masses m_{ν_i} through the famous see-saw formula [3–7]. With this set-up lepton-flavour violating (LFV) decays of charged leptons like $\ell_j \rightarrow \ell_i \gamma$ (where $\ell_{1,2,3} = e, \mu, \tau$) occur at unobservably small rates, because the transition amplitudes are suppressed by a factor of $(m_{\nu_j}^2 - m_{\nu_i}^2)/M_W^2$. This situation is dramatically different in the Minimal Supersymmetric Standard Model (MSSM), which contains new sources of flavour violation in the soft supersymmetry-breaking sector. To study LFV effects one commonly adopts a weak basis of the (s)lepton multiplets in which the lepton Yukawa couplings are flavour-diagonal. The off-diagonal elements of the charged slepton mass matrix, Δm_{XY}^{ij} with $i, j = 1, 2, 3$ and $X, Y = L, R$, give rise to LFV decays of charged leptons through loops containing a slepton and a neutralino. By confronting MSSM predictions with experimental upper bounds on LFV decay rates one can derive constraints on these elements, which are usually quoted for the dimensionless parameters

$$\delta_{XY}^{ij} = \frac{\Delta m_{XY}^{ij}}{\sqrt{m_{iX}^2 m_{jY}^2}}. \quad (1)$$

Here m_{iX} denotes the i -th diagonal element of the slepton mass matrix with chirality $X = L, R$. If all δ_{XY}^{ij} are small, m_{iX} essentially coincides with the corresponding physical i -th generation charged slepton mass. A different avenue to constrain the δ_{XY}^{ij} in Eq. (1) are studies of deviations from lepton flavour universality (LFU). This approach has been proposed in Ref. [8], which exploits the impressive experimental precision of

$$R_K = \frac{\Gamma(K \rightarrow e\nu)}{\Gamma(K \rightarrow \mu\nu)}. \quad (2)$$

This notation implies a sum over all three neutrino species. The experimental situation is summarised in Tab. 1. The cancellation of the hadronic uncertainties makes the theoretical prediction of R_K very clean: Including bremsstrahlung the SM value is given by [9–11]

$$R_K^{\text{SM}} = \frac{m_e^2 (m_K^2 - m_e^2)^2}{m_\mu^2 (m_K^2 - m_\mu^2)^2} (1 + \delta R_{\text{QED}}) = (2.477 \pm 0.001) \cdot 10^{-5} \quad (3)$$

The large helicity suppression of the SM contribution to the electronic decay mode makes R_K sensitive to effects of a charged Higgs boson. In the MSSM the charged-Higgs contribution cancels from R_K at tree-level. Yet, as pointed out in Ref. [8], at the loop level LFU-violating contributions involving Δm_{XY}^{ij} can lead to $R_K \neq R_K^{\text{SM}}$. It is convenient to parametrise the $\mu - e$ non-universality in R_K in terms of the quantity $\Delta r^{\mu-e}$ defined as

$$R_K = R_K^{\text{SM}} (1 + \Delta r^{\mu-e}). \quad (4)$$

Supersymmetric contributions which are linear in δ_{XY}^{ij} cannot interfere with the SM amplitude in $K \rightarrow \ell \nu_\ell$, because they lead to a final state with charged lepton and neutrino belonging to different fermion generations. Therefore these contributions will necessarily increase $\Gamma(K \rightarrow \ell \nu)$. In Ref. [8] a mechanism involving the product $\delta_{LL}^{13} \delta_{RR}^{13}$ has been proposed to achieve a suppression of $\Gamma(K \rightarrow e \nu_e)$ and therefore of R_K . Recently, two new observables have been found to constrain the very same combination of supersymmetric FCNC parameters [12]: Firstly, 't Hooft's naturalness criterion has

Experiment	$R_K [10^{-5}]$	error $\delta R_K/R_K$
PDG 2006	2.45 ± 0.11	4.5%
NA48/2 2003	$2.416 \pm 0.043 \pm 0.024$	2.8%
NA48/2 2004	$2.455 \pm 0.045 \pm 0.041$	3.5%
KLOE	$2.55 \pm 0.05 \pm 0.05$	3.9%
Kaon 2007	2.457 ± 0.032	1.3%
PDG 2008	2.447 ± 0.109	4.5%
PDG 2010	2.493 ± 0.036	1.4%
KLOE 2009	$2.493 \pm 0.025 \pm 0.019$	1.7%
NA62 Jan 2011	2.487 ± 0.013	0.5%
NA62 Jul 2011	2.488 ± 0.010	0.4%

Table 1: Experimental values for R_K [13–21]. We use the published result of Ref. [18] quoted in the second-to-last row, which corresponds to $\Delta r^{\mu-e} = 0.004 \pm 0.005$. The result in the last row, reported by NA62 at conferences [20, 21], corresponds to the full data set collected by NA62 in 2007–2008. For the future an experimental accuracy of $\delta R_K/R_K = 0.1 - 0.2\%$ is feasible for the NA62 experiment [17].

been applied to the electron mass yielding a non-decoupling upper bound on $|\delta_{LL}^{13} \delta_{RR}^{13}|$. Secondly, a powerful bound on $|\delta_{LL}^{13} \delta_{RR}^{13}|$ has been derived from the anomalous magnetic moment of the electron. The latter constraint decouples, i.e. becomes weaker for larger superpartner masses, but the bounds on $|\delta_{LL}^{13} \delta_{RR}^{13}|$ are comparable to the ones found from the electron mass for typical sparticle spectra. In Sect. 2 we use the results of Ref. [12] to assess the possible maximal effect on R_K from loop diagrams involving $\delta_{LL}^{13} \delta_{RR}^{13}$. In Sect. 3 we study MSSM contributions involving a single power of either δ_{LL}^{13} or δ_{RR}^{13} . These contributions feed $K \rightarrow e \nu_\tau$ and therefore increase R_K . In Sect. 4 we conclude.

2 Lepton-flavour conserving loop corrections

In a two-Higgs-doublet model of type II the following Hamiltonian describes leptonic Kaon decays [22]:

$$\mathcal{H} = \frac{G_F}{\sqrt{2}} V_{us} \left[\bar{u} \gamma^\mu (1 - \gamma^5) s \bar{\nu}_\ell \gamma_\mu (1 - \gamma^5) \ell - \frac{m_s m_\ell}{M_H^2} \tan^2 \beta \bar{u} (1 + \gamma^5) s \bar{\nu}_\ell (1 - \gamma^5) \ell \right] \quad (5)$$

yielding the decay rate

$$\Gamma(K \rightarrow \ell \nu_\ell) = \frac{G_F^2}{8\pi} m_\ell^2 m_K f_K^2 |V_{us}|^2 \left(1 - \frac{m_\ell^2}{m_K^2} \right)^2 \left[1 - m_K^2 \frac{\tan^2 \beta}{M_H^2} \right]^2, \quad \ell = e, \mu \quad (6)$$

where the second contribution in the square brackets stems from the additional charged-Higgs exchange. At tree level the relative Higgs contribution to the decay rate is independent of the lepton flavour and thus cancels in the ratio R_K defined in Eq. (2). However, SUSY loop corrections can introduce a dependence on the lepton flavour: In the large $\tan \beta$ regime of the MSSM the relation between the Yukawa couplings and the measured fermion masses can change significantly, with the loop

suppression compensated by a factor of $\tan \beta \sim 50$. In the decoupling limit $M_{\text{SUSY}} \gg v, M_H$ these enhanced corrections arise in a very intuitive way from a loop-induced non-holomorphic Higgs coupling [23]. (Here $\tan \beta = v_u/v_d$ denotes the ratio of the two Higgs vevs, $v = \sqrt{v_u^2 + v_d^2} = 174 \text{ GeV}$ is the electroweak scale, M_H represents the charged-Higgs boson mass, and M_{SUSY} is the mass scale of the supersymmetric particles entering the loop diagrams.) In our case of lepton Yukawa couplings the applicability of the decoupling limit is not clear a priori, because some of the superpartners involved (e.g. neutralinos) can easily have masses around or even below v . To cover the case $M_{\text{SUSY}} \sim v, M_H$ one must resort to a diagrammatic resummation of $\tan \beta$ -enhanced corrections, which has been worked out for quarks in Refs. [24, 25] and for leptons in Refs. [12, 26]. The desired all-order relation between the Yukawa coupling y_ℓ and the physical lepton mass m_ℓ is

$$-y_\ell v_d = m_\ell + \Sigma_\ell - \Sigma_\ell^2 + \Sigma_\ell^3 - \dots \quad (7)$$

where Σ_ℓ is the piece of the one-loop self-energy proportional to $m_\ell \tan \beta$. In the on-shell renormalisation scheme the mass counterterm is just $\delta m_\ell = \Sigma_\ell$ up to terms which are not enhanced by a factor of $\tan \beta$. Eq. (7) is conventionally written as

$$-y_\ell \sin \beta = \frac{m_\ell \tan \beta}{v(1 + \epsilon_\ell \tan \beta)} = \frac{g_2}{\sqrt{2}M_W} \frac{m_\ell \tan \beta}{1 + \epsilon_\ell \tan \beta}, \quad \epsilon_\ell \tan \beta = -\frac{\Sigma_\ell}{m_\ell}. \quad (8)$$

$-y_\ell \sin \beta$ is just the Higgs coupling to right-handed down-type leptons contributing to the second terms in the square brackets in Eqs. (5) and (6). Putting everything together one finds

$$R_K = R_K^{\text{SM}} \left[\frac{1 - m_K^2 \frac{\tan^2 \beta}{M_H^2} \frac{1}{(1 + \epsilon_s \tan \beta)(1 + \epsilon_e \tan \beta)}}{1 - m_K^2 \frac{\tan^2 \beta}{M_H^2} \frac{1}{(1 + \epsilon_s \tan \beta)(1 + \epsilon_\mu \tan \beta)}} \right]^2, \quad (9)$$

where ϵ_s is the analogue of ϵ_ℓ for the strange Yukawa coupling. This reads

$$\Delta r^{\mu-e} = -\frac{2m_K^2 \tan^2 \beta}{M_H^2 |1 + \epsilon_s \tan \beta|} \left[\frac{1}{|1 + \epsilon_e \tan \beta|} - \frac{1}{|1 + \epsilon_\mu \tan \beta|} \right] \quad (10)$$

in terms of the notation of Eq. (4). Lepton universality is violated for $\epsilon_e \neq \epsilon_\mu$. In the MSSM with minimal flavour violation (MFV) the only source of $\epsilon_e \neq \epsilon_\mu$ are different values of the selectron and smuon masses. A sizable slepton mass splitting between the first and second generation is theoretically hard to justify and we do not consider this possibility any further.

An a priori sizable source of lepton non-universality are the diagrams involving a double insertion of LFV mass insertions [8], see Fig. 1¹. Instead of the tree level coupling which is proportional to $m_e \tan \beta$ the diagram gives a contribution proportional to $m_\tau \tan \beta$. This is the dominant contribution to the LFC self energy through double LFV and is given as (with the notation and conventions explained in Appendices A, B of Ref. [12])²:

$$\Sigma_e^{FV} = \frac{\alpha_1}{4\pi} \mu M_1 m_{\tilde{e}_L} m_{\tilde{e}_R} m_{\tilde{\tau}_L} m_{\tilde{\tau}_R} \delta_{LL}^{13} \delta_{RR}^{13} \frac{m_\tau \tan \beta}{1 + \epsilon_\tau \tan \beta} F_0(M_1^2, m_{\tilde{e}_L}^2, m_{\tilde{e}_R}^2, m_{\tilde{\tau}_L}^2, m_{\tilde{\tau}_R}^2). \quad (11)$$

¹The SU(2) partner diagram of Fig. 1 involving a charged Higgs boson was shown in Ref. [8].

²Interchanging the chiralities of the two $\tilde{\tau}$ yields the analogous expression with $\delta_{LR}^{13} \delta_{LR}^{31}$.

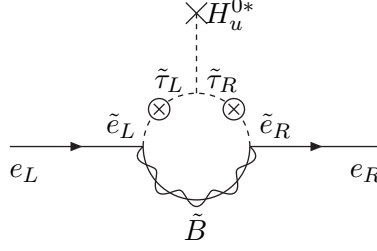


Figure 1: Dominant double LFV contribution to the electron mass renormalisation.

Throughout this paper we choose μ , the gaugino mass parameters, the trilinear SUSY breaking terms, and all off-diagonal slepton mass matrix elements real. Therefore $\epsilon_s, \epsilon_\ell$ are real as well. Eq. (11) describes a non-decoupling effect, because $F_0 \propto M_{\text{SUSY}}^{-6}$. The contribution of Σ_e^{FV} to the resummation formulae in Eq. (8) is [12]:

$$-y_e \sin \beta = \frac{g_2}{\sqrt{2}M_W} \frac{(m_e + \Sigma_e^{FV}) \tan \beta}{1 + \epsilon_e \tan \beta}. \quad (12)$$

Writing

$$\Sigma_e^{FV} \equiv \frac{m_\tau \tan \beta}{1 + \epsilon_\tau \tan \beta} \Delta_{LR}^e \quad (13)$$

to adopt a notation similar to Ref. [8] the charged-Higgs coupling to the electron changes to

$$-y_e \sin \beta = \frac{ig_2}{\sqrt{2}M_W} \frac{m_e}{1 + \epsilon_e \tan \beta} \tan \beta \left(1 + \frac{\Sigma_e^{FV}}{m_e} \right) \quad (14)$$

$$= \frac{ig_2}{\sqrt{2}M_W} \frac{m_e}{1 + \epsilon_e \tan \beta} \tan \beta \left(1 + \frac{m_\tau}{m_e} \frac{\tan \beta}{1 + \epsilon_\tau \tan \beta} \Delta_{LR}^e \right). \quad (15)$$

Recalling the discussion after Eq. (7) we see that there is a one-to-one correspondence between the electron mass counterterm Σ_e^{FV} and the enhanced Yukawa coupling in Eq. (14). In Ref. [12] 't Hooft's naturalness criterion has been applied to the electron mass to derive a bound on $|\Sigma_e^{FV}|$: Within theories with MFV the smallness of m_e is justified by the chiral symmetry gained in the limit $y_e \rightarrow 0$. In our case a second symmetry-breaking parameter, $y_\tau \delta_{LL}^{13} \delta_{RR}^{13}$ is present, and the naturalness principle forbids large accidental cancellations between the two contributions to m_e . Demanding $|\Sigma_e^{FV}| \lesssim m_e$ one finds the bounds in Tab. 2 [12], which can be summarised as

$$|\delta_{LL}^{13} \delta_{RR}^{13}| \lesssim 0.1. \quad (16)$$

The authors of Ref. [8] have used $\Delta_{LR}^e = \mathcal{O}(10^{-4})$ to bring R_K into better agreement with the NA48/2 result of 2004, see Tab. 1. This value implies a 2000% change in the electron mass which is incompatible with the naturalness principle.

After considering the MSSM we turn our argument into a model-independent analysis: For the naturalness bound on y_e it is inessential in which theory the self-energy Σ_e^{FV} is calculated. Any theory

with a tree-level Higgs sector corresponding to a type-II 2HDM and a self-energy contribution Σ_e^{FV} not proportional to y_e affects the charged-Higgs coupling through the finite counterterm

$$\delta y_e = \frac{y_e}{m_e} \delta m_e = \frac{y_e}{m_e} \frac{\Sigma_e^{FV} - \epsilon_e \tan \beta}{1 + \epsilon_e \tan \beta} \simeq \frac{y_e}{m_e} \Sigma_e^{FV}. \quad (17)$$

If we take the upper bound from the fine tuning argument $|\delta m_e| = m_e$, the allowed range for y_e lies between 0 and twice the tree-level value m_e/v_d . The largest allowed value for $-\Delta r^{\mu-e}$ in Eq. (4) therefore corresponds to

$$\Delta r_{\min, \text{LFC}}^{\mu-e} = -4 \frac{m_K^2 \tan^2 \beta}{M_H^2 (1 + \epsilon_s \tan \beta)}. \quad (18)$$

This bound assumes that (as in the MSSM) the muon Yukawa coupling is not substantially affected. Taking $\tan \beta = 50$, $\epsilon_s \tan \beta = 0.3$ (which corresponds to a typical loop suppression factor $\epsilon_s = \frac{1}{16\pi^2}$ and $\tan \beta = 50$), and a charged-Higgs mass of $M_H = 300$ GeV we find $\Delta r_{\min, \text{LFC}}^{\mu-e} = -5 \cdot 10^{-3}$, which can be probed by NA62 but is not in the 5σ discovery reach of this experiment. Of course our consideration equally applies to positive values of $\Delta r_{\min, \text{LFC}}^{\mu-e}$, i.e. the naturalness bound implies $|\Delta r_{\text{LFC}}^{\mu-e}| \leq 5 \cdot 10^{-3}$. We have discussed negative contributions, because $\Delta r^{\mu-e} < 0$ is an unambiguous sign of an LFC mechanism, while $\Delta r^{\mu-e} > 0$ can be more easily accommodated with LFV new physics as analysed in Sect. 3. In Ref. [27] (which is an update of Ref. [8]) a thorough analysis of several observables in quark and lepton flavour physics has been performed. While most of the points in the scatter plots of that paper satisfy the constraint from Eq. (18), an inclusion of Eq. (16) into the analysis would eliminate the outliers in these plots. Further the use of Eq. (16) would make the results of Ref. [27] less dependent on the anomalous magnetic moment of the muon, whose theoretical prediction in the SM involves uncertainties which are not fully understood.

We note that $|\delta_{LL}^{13} \delta_{RR}^{13}|$ can also be bounded in a completely different way: The anomalous magnetic moment of the *electron* gives essentially the same bound as Eq. (16) for $M_{\text{SUSY}} = 500$ GeV and involves the same supersymmetric particles in the loop as Σ_e^{FV} as shown in Ref. [12]. Thus relaxing the naturalness bound $|\Sigma_e^{FV}| \leq m_e$ to lower $\Delta r_{\min, \text{LFC}}^{\mu-e}$ in Eq. (18) requires the choice of larger bino or selectron masses to comply with the electron magnetic moment. Should future NA62 data point towards $\Delta r^{\mu-e} < 0$, an analysis in conjunction with the electron magnetic moment will place correlated lower bounds on these particle masses.

While NA62 is gaining statistics in the forthcoming years, we may expect increasingly better information on M_H and $\tan \beta$ from LHC experiments, so that the bound $\Delta r_{\min, \text{LFC}}^{\mu-e} = -5 \cdot 10^{-3}$ quoted after Eq. (18) may eventually become tighter. Any future NA62 measurement of $\Delta r^{\mu-e}$ below $\Delta r_{\min, \text{LFC}}^{\mu-e}$ will then establish a more exotic new physics explanation than type-II charged-Higgs exchange, such as t-channel leptoquark exchange.

3 Lepton-flavour violating loop corrections

Flavour-violating self-energies in the charged-lepton line can induce the decays $K \rightarrow \ell \nu_{\ell'}$ with $\ell \neq \ell'$ [8]. A sizable effect is only possible in $K \rightarrow e \nu_\tau$, so that LFV self-energies can only increase R_K . In this section we estimate the maximal effect of lepton-flavour violating loop corrections to R_K . A large correction to R_K involves large $\tilde{\tau}_L$ - $\tilde{\tau}_R$ mixing. We cannot rely on the expansion in v^2/M_{SUSY}^2 adopted in Ref. [8, 27] in this region of the MSSM parameter space, because the $\tilde{\tau}$ mixing angle θ_τ vanishes for $v/M_{\text{SUSY}} \rightarrow 0$. We use the exact formulae of Ref. [12], which express $\Delta r^{\mu-e}$ in terms

scenario		$x = 0.3$	$x = 1$	$x = 1.5$	$x = 3.0$	for
1	$M_1 = M_2 = m_L = m_R$	0.261	0.073	0.050	0.026	$\delta_{RR}^{13} \delta_{LL}^{13} > 0$
		0.234	0.059	0.040	0.023	$\delta_{RR}^{13} \delta_{LL}^{13} < 0$
2	$3M_1 = M_2 = m_L = m_R$	0.301	0.083	0.057	0.029	$\delta_{RR}^{13} \delta_{LL}^{13} > 0$
		0.269	0.067	0.045	0.024	$\delta_{RR}^{13} \delta_{LL}^{13} < 0$
3	$M_1 = M_2 = 3m_L = m_R$	0.292	0.082	0.057	0.031	$\delta_{RR}^{13} \delta_{LL}^{13} > 0$
		0.235	0.067	0.042	0.027	$\delta_{RR}^{13} \delta_{LL}^{13} < 0$
4	$M_1 = M_2 = \frac{m_L}{3} = m_R$	0.734	0.210	0.142	0.071	$\delta_{RR}^{13} \delta_{LL}^{13} > 0$
		0.702	0.190	0.127	0.064	$\delta_{RR}^{13} \delta_{LL}^{13} < 0$
5	$3M_1 = M_2 = m_L = 3m_R$	0.731	0.205	0.137	0.067	$\delta_{RR}^{13} \delta_{LL}^{13} > 0$
		0.693	0.179	0.116	0.054	$\delta_{RR}^{13} \delta_{LL}^{13} < 0$

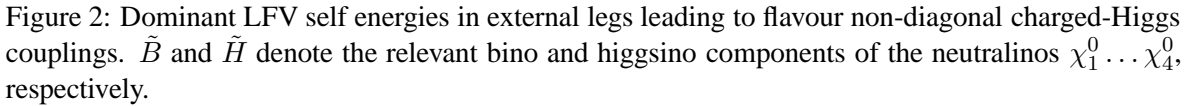
Table 2: Different mass scenarios and the corresponding upper bounds for $|\delta_{RR}^{13} \delta_{LL}^{13}|$. $m_{R,L}$ denotes the average right and left-handed slepton mass, respectively, M_1 and M_2 the bino and wino masses and $x = \mu/m_R$. In all scenarios, $\tan \beta = 50$ and $\text{sgn } \mu = +1$.

of the masses of the physical stau eigenstates $\tilde{\tau}_{1,2}$ rather than the diagonal elements $m_{\tilde{\tau}_{L,R}}^2$ of the stau mass matrix. Since NA62 runs concurrently with the LHC, it is anyway useful to express $\Delta r^{\mu-e}$ in terms of the physical quantities probed in high- p_T physics.

$\Sigma_{\ell_{jR}-\ell_{iL}}$ is relevant for the W -coupling to leptons if $j > i$ (and thus contributes to threshold corrections of the PMNS matrix as studied in Ref. [12,28]), whereas for $j < i$ $\Sigma_{\ell_{jR}-\ell_{iL}}$ is responsible for the correction of the charged-Higgs coupling. The charged-Higgs couplings to leptons $\Gamma_{\ell_i \nu_{\ell_j}}^{H^+}$ including an analytic resummation of $\tan \beta$ -enhanced corrections are listed in Eqs. (31a-c), (32a-c) and (33a-c) of Ref. [12]. For the decoupling limit $M_{\text{SUSY}} \gg v$ these charged-Higgs couplings were derived earlier in Eqs. (92-95) of Ref. [29], which further uses the iterative procedure of Ref. [30] to resum the $\tan \beta$ -enhanced terms. In this paper we are interested in the $\tau_L \rightarrow e_R$ self-energy contributing to R_K as shown in Fig. 2, aiming at constraints on δ_{RR}^{31} to be obtained from future NA62 data. With the LFV Higgs couplings at hand one can calculate the decay rates summing over all neutrino species and compute the ratio. The $H^+ e \nu_\tau$ vertex, which involves the enhancement factor of m_τ/m_e , is the only relevant contribution to R_K : Corrections to the muonic decay mode are irrelevant due to the much smaller enhancement factor of m_τ/m_μ . In view of the result of the previous section we can further rule out large effects in $\Gamma_{e\nu_e}^{H^+}$. In the LFV case the deviation from the SM is essentially given as:

$$\Delta r_{\text{LFV}}^{\mu-e} = \frac{m_K^4 \tan^4 \beta}{M_H^4 (1 + \epsilon_s \tan \beta)^2 (1 + \epsilon_\tau \tan \beta)^2} \frac{m_\tau^2}{m_e^2} \left[\frac{\Sigma_{\tau_L-e_R}^{\tilde{\chi}^0}}{m_\tau} \right]^2. \quad (19)$$

Here $\Sigma_{\tau_L-e_R}^{\tilde{\chi}^0}$ denotes the sum of the two self-energies appearing in Fig. 2. For the $\tau_L \rightarrow e_R$ -transition only the two diagrams in Fig. 2 are not suppressed with y_e . We explicitly account for stau mixing with mixing angle $\theta_\tau \in [-\pi/4, \pi/4]$ and stau mass eigenstates $\tilde{\tau}_1 = \tilde{\tau}_L \cos \theta_\tau - \tilde{\tau}_R \sin \theta_\tau$, $\tilde{\tau}_2 = \tilde{\tau}_L \sin \theta_\tau + \tilde{\tau}_R \cos \theta_\tau$. We use the following identities (with $m_\tau^{(0)} = m_\tau/(1 + \epsilon_\tau \tan \beta)$) and the


$$\sin(2\theta_\tau) = \frac{2\Delta m_{LR}^{33}}{m_{\tilde{\tau}_1}^2 - m_{\tilde{\tau}_2}^2} = \frac{-2m_\tau^{(0)}\mu \tan\beta}{m_{\tilde{\tau}_1}^2 - m_{\tilde{\tau}_2}^2}, \quad \cos(2\theta_\tau) = \frac{m_{\tilde{\tau}_L}^2 - m_{\tilde{\tau}_R}^2}{m_{\tilde{\tau}_1}^2 - m_{\tilde{\tau}_2}^2} \quad (20)$$

$$\text{sgn}(m_{\tilde{\tau}_1}^2 - m_{\tilde{\tau}_2}^2) = \text{sgn}(m_{\tilde{\tau}_L}^2 - m_{\tilde{\tau}_R}^2) \quad (22)$$

$$m_{\tilde{\tau}_1} = m_{\tilde{\tau}_2} - \frac{2\mu m_\tau^{(0)} \tan \beta}{\sin(2\theta_\tau)}. \quad (23)$$
$$m_{\tilde{\tau}_L}^2 = m_{\tilde{\tau}_l}^2 + \frac{\mu m_\tau^{(0)} \tan \beta}{|\sin(2\theta_\tau)|} (1 - \text{sgn}(\theta_\tau) \cos(2\theta_\tau)) , \quad (24)$$

The phenomenologically interesting large values of $\Delta r^{\mu-e}$ involve large values of $|\mu|$. Varying $|\mu|$ to larger values with $m_{\tilde{\tau}_{L,R}}^2$ fixed increases the mass splitting between the two stau mass eigenstates $\tilde{\tau}_l$ and $\tilde{\tau}_h$ and will eventually lower the smaller physical stau mass $m_{\tilde{\tau}_l}$ below its experimental lower bound. We avoid this problem by varying the parameters for fixed $m_{\tilde{\tau}_l}$. Treating the flavour violating off-diagonal elements up to linear order and including stau mixing we get for the left diagram in Fig. 2:

Here and in the following we need the loop functions

$$f_1(x,y,z) = \frac{xy \ln \frac{x}{y} + xz \ln \frac{z}{x} + yz \ln \frac{y}{z}}{(x-y)(x-z)(y-z)}, \quad f_2(x,y,z,w) = \frac{f_1(x,y,z) - f_1(x,y,w)}{z-w}. \quad (27)$$

For the right diagram in Fig. 2 we get the following contribution:

$$\begin{aligned} \Sigma_{\tau_L-e_R}^{\tilde{H}-\tilde{B}} &= \frac{\alpha_1}{4\pi} \frac{m_\tau \tan \beta}{1 + \epsilon_\tau \tan \beta} M_1 \mu m_{\tilde{e}_R} m_{\tilde{\tau}_R} \delta_{RR}^{13} \cdot \\ &\cdot \left[\sin^2 \theta_\tau f_2(M_1^2, \mu^2, m_{\tilde{\tau}_1}^2, m_{\tilde{e}_R}^2) + \cos^2 \theta_\tau f_2(M_1^2, \mu^2, m_{\tilde{\tau}_2}^2, m_{\tilde{e}_R}^2) \right]. \end{aligned} \quad (28)$$

In order not to get negative slepton masses, $|\delta_{RR}^{13}|$ must for sure be smaller than 1. Here, we only consider a single flavour-violating mass insertions. Contributions with double mass insertion, e.g. $\delta_{LL}^{23} \delta_{RR}^{13*}$ can be relevant for $\mu \rightarrow e\gamma$ [31]. In principle, $\Sigma_{\tau_L-e_R}^{\tilde{X}^0} = \Sigma_{\tau_L-e_R}^{\tilde{B}} + \Sigma_{\tau_L-e_R}^{\tilde{H}-\tilde{B}}$ is sensitive to the RR-element. However, the relative minus sign is the origin of a possible cancellation in certain region of the parameter space. In this approximation the sensitivity to δ_{RR}^{13} vanishes if $\mu^2 = m_{\tilde{\tau}_1}^2 \cos^2 \theta_\tau + m_{\tilde{\tau}_2}^2 \sin^2 \theta_\tau$. In the case with $\theta_\tau = 0$ the cancellation occurs for $\mu^2 = m_{\tilde{\tau}_L}^2$. This feature was already discovered in Ref. [32]. In Refs. [8, 27] the decoupling limit $M_{\text{SUSY}} \gg v$ is adopted. In this limit $\tilde{\tau}_{L,R}$ appear in the loop functions instead of $\tilde{\tau}_{1,2}$ and the $\tilde{\tau}_L-\tilde{\tau}_R$ flip in the bino diagram is incorporated within the mass insertion approximation (MIA). This results in a simplified version of our Eqs. (26) and (28); in Eq. (28) the square bracket simplifies to $f_2(M_1^2, \mu^2, m_{\tilde{\tau}_R}^2, m_{\tilde{e}_R}^2)$.³ Since θ_τ vanishes for $M_{\text{SUSY}} \gg v$, the consideration of large stau mixing requires to go beyond the decoupling limit and beyond MIA. Furthermore the stau and bino masses can still be smaller than v ; in fact the interesting region of the parameter space probed by NA62 comes with light bino and staus.

We now estimate the maximal allowed LFV effect in R_K including stau mixing, which depends very much on $\mu \tan \beta$. At the end of Sect. 2 we already concluded that effective LFC effects are typically below the experimental sensitivity. In our plots and numerical examples we use the following values for the smaller stau mass $m_{\tilde{\tau}_l}$ and the bino mass parameter M_1 :

$$m_{\tilde{\tau}_l} = 120 \text{ GeV}, \quad M_1 = 100 \text{ GeV} \quad (29)$$

These values are consistent with the experimental lower bounds of 46 GeV for the neutralino masses and 81.9 GeV for $m_{\tilde{\tau}_l}$ [13]. The heavier stau mass $m_{\tilde{\tau}_h}$ is then calculated from the mixing angle θ_τ and μ . For the off-diagonal element $\Delta m_{RR}^{13} = m_{\tilde{e}_R} m_{\tilde{\tau}_R} \delta_{RR}^{13}$ we choose for simplification $m_{\tilde{e}_R} = 200 \text{ GeV}$, with $m_{\tilde{\tau}_R}$ also calculated from θ_τ , μ , and $m_{\tilde{\tau}_l}$. With this choice the bino diagram increases with μ , since $m_{\tilde{\tau}_R}$ and $m_{\tilde{\tau}_h}$ increase too. (Setting instead $\Delta m_{RR}^{13} = m_{\tilde{e}_R}^2 \delta_{RR}^{13}$ would lead to a finite limit for $\Sigma_{\tau_L-e_R}^{\tilde{B}}$ for $\mu \rightarrow \infty$.) Furthermore, we choose $\tan \beta = 50$ and μ to be real and positive. With this chosen input parameters we can analyse the dependence of $\Delta r^{\mu-e}$ on θ_τ , μ and δ_{RR}^{13} . For small values of μ the higgsino-bino diagram dominates, but the maximal value is rather small. For large μ (and other SUSY masses fixed) the higgsino-bino diagram tends to zero whereas the pure bino-diagram can become sizeable. Without stau mixing this diagram would not contribute at all. Thus, in order to get any sizeable effect, especially for large values of μ , one has to take stau mixing into account. With this setup the largest effect in $\Sigma_{\tau_L-e_R}^{\tilde{B}}/m_\tau$ comes with a relatively large mixing angle of $\theta_\tau \approx 26^\circ$. In case of the higgsino-bino diagram, stau mixing is not important, this diagram is maximal for small μ , but nevertheless approximately one order of magnitude smaller than the largest values found for the pure bino diagram. For $\theta_\tau \approx 26^\circ$ and $\mu > 0$ one has $\tilde{\tau}_l = \tilde{\tau}_1$, which moreover is dominantly left-handed.

The maximal possible deviation of R_K from the SM prediction is visualized in Fig. 3 where $\Delta r^{\mu-e}$ is plotted for $\delta_{RR}^{13} = 0.5$, $M_H = 500 \text{ GeV}$ and $\tan \beta = 50$ as a function of θ_τ and μ using typical

³The relation between the notation in Ref. [8, 27] and ours is $\Sigma_{\tau_L-e_R}^{\tilde{X}^0} = \frac{m_\tau \tan \beta}{1 + \epsilon_\tau \tan \beta} \Delta_{RR}^{3e}$. E.g. the second term in Δ_{RR}^{3e} corresponds to the bino diagram with the following simplification compared to Eq. (26): $\sin \theta_\tau \cos \theta_\tau (f_1(M_1^2, m_{\tilde{e}_R}^2, m_{\tilde{\tau}_1}^2) - f_1(M_1^2, m_{\tilde{e}_R}^2, m_{\tilde{\tau}_2}^2)) \approx f_1'(M_1^2, m_{\tilde{e}_R}^2, m_{\tilde{\tau}_R}^2)$.

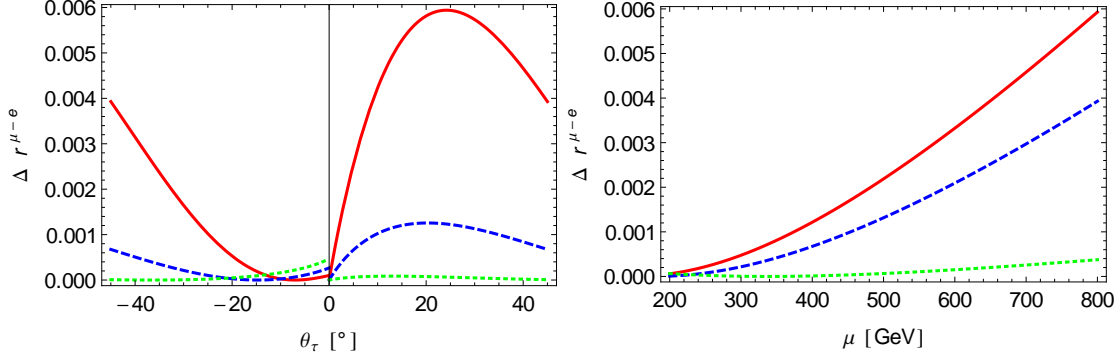


Figure 3: $\Delta r^{\mu-e}$ for $\delta_{RR}^{13} = 0.5$, $M_H = 500$ GeV and $\tan \beta = 50$. Left: As a function of θ_τ for different values of μ : 800 GeV (red), 400 GeV (blue dashed), 200 GeV (green dotted). Right: In dependence of μ for different values of θ_τ : 26° (red), 45° (blue dashed), -18° (green dotted).

values of $\epsilon_s \tan \beta = 0.3$ and $\epsilon_e \tan \beta = \epsilon_\tau \tan \beta = -0.07$. The discontinuity at $\theta_\tau = 0$ just comes from the fact that $\tilde{\tau}_1$ and $\tilde{\tau}_2$ change their roles as heavier and lighter staus. In order to find $\Delta r^{\mu-e}$ for different values of δ_{RR}^{13} , M_H and $\tan \beta$ one must rescale those plots using that $\Delta r^{\mu-e}$ is quadratic in δ_{RR}^{13} , $\propto M_H^{-4}$ and $\propto \tan^6 \beta$. One gets a maximal effect of 0.6% for our chosen point of $\mu = 800$ GeV, $M_H = 500$ GeV, $\delta_{RR}^{13} = 0.5$, $\theta_\tau = 26^\circ$ and $\tan \beta = 50$, which is already in the reach of NA62. In the range of $500 \text{ GeV} \leq \mu \leq 900 \text{ GeV}$ a handy approximate formula (with an error of 7%) for the maximal effect (occurring at $\theta_\tau = 26^\circ$) can be found

$$\Delta r_{\text{max,LFV}}^{\mu-e} \approx 0.006 \left(\frac{500 \text{ GeV}}{M_H} \right)^4 \left(\frac{\tan \beta}{50} \right)^6 \left(\frac{\delta_{RR}^{13}}{0.5} \right)^2 \left(\frac{\mu}{800 \text{ GeV}} \right)^2.$$

valid for $m_{\tilde{\tau}_1} = 120$ GeV, $M_1 = 100$ GeV, $m_{\tilde{e}_R} = 200$ GeV. (30)

If one varies the lightest stau mass, $\Delta r^{\mu-e}$ scales approximately as $(120 \text{ GeV}/m_{\tilde{\tau}_1})^2$ in the range $100 \text{ GeV} \leq m_{\tilde{\tau}_1} \leq 250 \text{ GeV}$. The dependence on M_1 is roughly linear for $50 \text{ GeV} \leq M_1 \leq 100 \text{ GeV}$ and the prefactor in Eq. (30) decreases from 0.006 to 0.0028 if M_1 is lowered to 50 GeV. Above 100 GeV the M_1 dependence flattens off with a maximum at 200 GeV, at which the prefactor of our approximate formula becomes 0.0078. A full investigation of the dependences of $\Delta r^{\mu-e}$ on M_1 and $m_{\tilde{e}_R}$ requires the use of the exact expression, obtained by adding the quantities in Eqs. (28) and (26) to find $\Sigma_{\tau_L-e_R}^{\chi^0}$ and inserting the result into $\Delta r^{\mu-e}$ in Eq. (19).

In Fig. 4 we show the dependence of $\Delta r^{\mu-e}$ on μ , M_H , $\tan \beta$ and δ_{RR}^{13} for $\theta_\tau = 26^\circ$. It is possible to reach an effect of $\mathcal{O}(0.5\%)$, whereas for vanishing mixing or small μ it is hardly possible to reach the experimental sensitivity. To derive constraints on δ_{RR}^{13} Fig. 5 might be useful. We show regions in the $(M_H, \mu, \tan \beta, \delta_{RR}^{13})$ parameter space where $\Delta r^{\mu-e}$ reaches the future experimental sensitivity of 0.2%. In Ref. [12] it is pointed out that even large values of $\tan \beta = 100$ are compatible with the requirement of perturbative bottom Yukawa coupling.

In order to estimate the contribution of $\tau_L \rightarrow e_R$ transition to R_K in Ref. [8], the authors used $\Delta_R^{31} = 5 \cdot 10^{-4}$ which is related to our notation by $\Sigma_{\tau_L-e_R} = \frac{m_\tau \tan \beta}{1 + \epsilon_\tau \tan \beta} \Delta_R^{31}$ or $|\Sigma_{\tau_L-e_R}^{\tilde{\chi}^0}|/m_\tau = 0.025$. However, such large values correspond to quite specific points in the MSSM parameter space, especially extremely large μ . Thus, in order not to overestimate the effect and to avoid trouble with too small slepton masses one should rather take at most $|\Sigma_{\tau_L-e_R}^{\tilde{\chi}^0}|/m_\tau \approx 0.01$ (meaning $\Delta_{R,\text{max}}^{31} =$

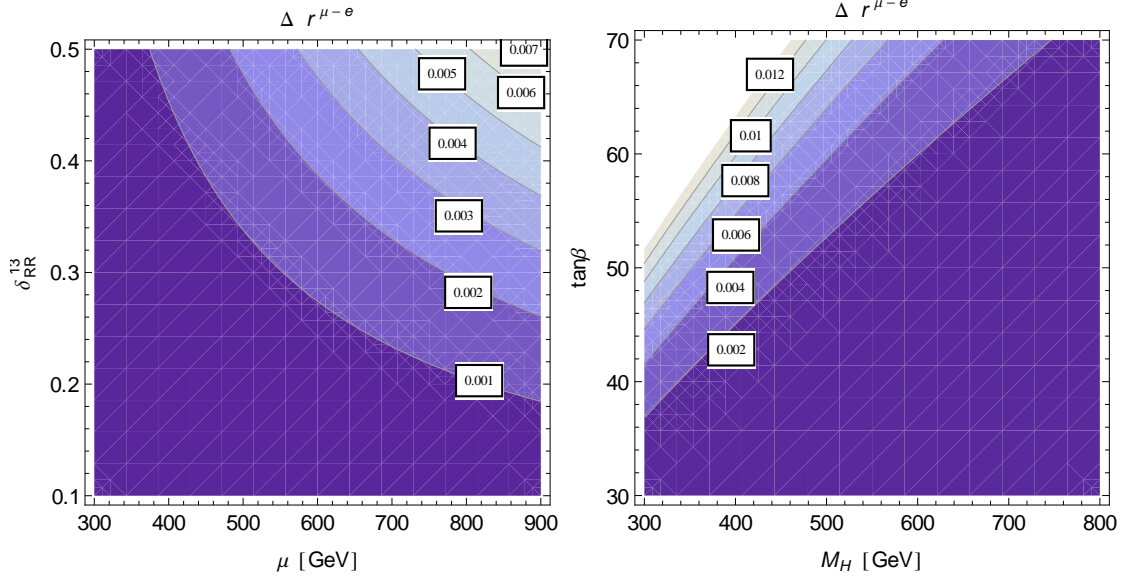


Figure 4: $\Delta r^{\mu-e}$ as a function of μ , δ_{RR}^{13} , M_H and $\tan\beta$ and stau mixing angle $\theta_\tau = 26^\circ$. Left: $M_H = 500$ GeV and $\tan\beta = 50$. Right: $\mu = 800$ GeV and $\delta_{RR}^{13} = 0.25$.

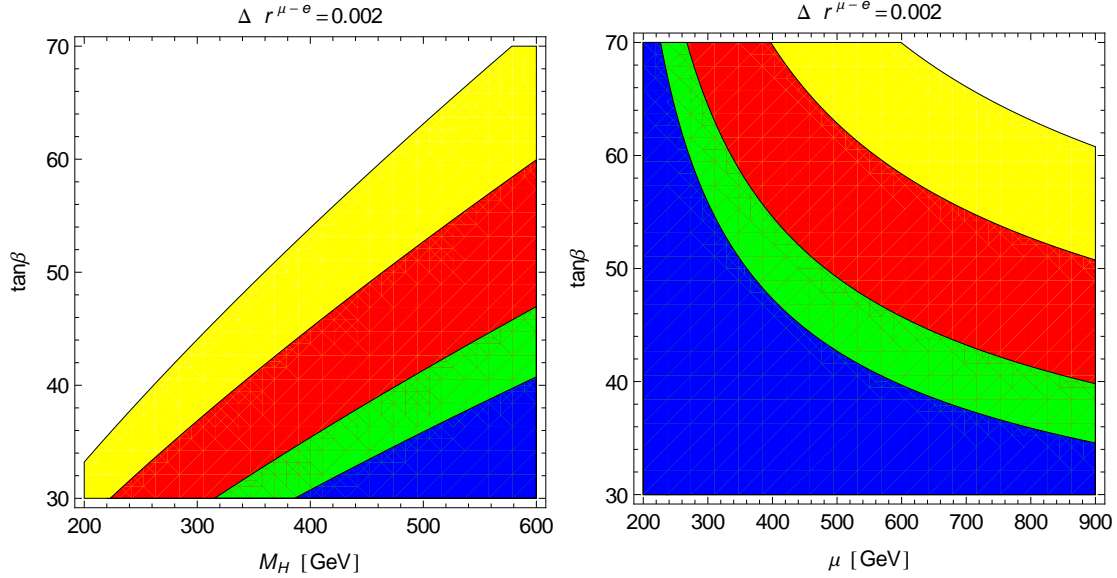


Figure 5: For different values of $\delta_{RR}^{13} = 0.15$ (yellow), 0.25 (red), 0.5 (green), 0.75 (blue) (from top to bottom) we plot the regions in which $\Delta r^{\mu-e}$ is below the future experimental sensitivity of 0.002 in the M_H - $\tan\beta$ plane with $\mu = 800$ GeV (left) and in the μ - $\tan\beta$ plane with $M_H = 500$ GeV (right) and stau mixing angle $\theta_\tau = 26^\circ$. I.e. if $\delta_{RR}^{13} = 0.25$, the white and yellow areas correspond to $\Delta r^{\mu-e} \geq 0.002$.

$2 \cdot 10^{-4}$). Taking this maximal value and further $\tan \beta = 50$ and a charged-Higgs mass of $M_H = 500$ GeV we end up with $\Delta r_{\text{max,LFV}}^{\mu-e} \approx 0.007$, which is within the experimental sensitivity of the NA62 experiment.

In Ref. [19] the 95%CL exclusion region for R_K for three different values of Δ_R^{31} ($1 \cdot 10^{-3}, 5 \cdot 10^{-4}, 1 \cdot 10^{-4}$) is shown in the $(M_{H^\pm}, \tan \beta)$ region and compared with the constraints from $B \rightarrow \tau \nu$, $B \rightarrow X_s \gamma$, $R_{\mu 23} = \Gamma(K \rightarrow \mu \nu) / \Gamma(K \rightarrow \pi^0 \mu \nu)$ [33] and direct H^\pm searches. According to the discussion in the preceding paragraph we prefer to take $\Delta_R^{31} = 2 \cdot 10^{-4}$ as the maximal value, so that our excluded $(M_{H^\pm}, \tan \beta)$ region is smaller than the one in Ref. [19]. In the following we use [34–37]

$$\mathcal{B}(B \rightarrow \tau \nu)^{\text{SM}} = 1.13 \cdot 10^{-4} \left(\frac{|V_{ub}|}{4 \cdot 10^{-3}} \right)^2 \left(\frac{f_B}{200 \text{ MeV}} \right)^2, \quad (31)$$

$$\mathcal{B}(B \rightarrow \tau \nu)^{\text{exp}} = (1.64 \pm 0.34) \cdot 10^{-4}, \quad (32)$$

$$\mathcal{B}(B \rightarrow \tau \nu)^{\text{SUSY}} = \left[1 - \left(\frac{m_B}{m_{H^+}} \right)^2 \frac{\tan^2 \beta}{(1 + \epsilon_0 \tan \beta)(1 + \epsilon_\tau \tan \beta)} \right]^2 \mathcal{B}(B \rightarrow \tau \nu)^{\text{SM}} \quad (33)$$

with $\epsilon_0 \approx \epsilon_s \approx \frac{1}{16\pi^2} \epsilon_\tau \tan \beta = -0.07$ and $\mu = 800$ GeV as above. In Fig. 6 we plot the region in the $M_{H^\pm} - \tan \beta$ plane satisfying $\Delta r^{\mu-e} \leq 0.5\%$ for three different values of δ_{RR}^{13} (0.15, 0.25, 0.5). Overlaid are the constraints from $B \rightarrow \tau \nu$, $R_{\mu 23} = \Gamma(K \rightarrow \mu \nu) / \Gamma(K \rightarrow \pi^0 \mu \nu)$ and direct H^\pm searches. The prediction of $\mathcal{B}(B \rightarrow \tau \nu)$ within the SM and the MSSM requires the knowledge of $|V_{ub}|$. Determinations of $|V_{ub}|$ from different quantities result in substantially different numerical predictions. For discussions of this “ V_{ub} -puzzle” see Refs. [34, 37, 38]. For our analysis we consider two extreme scenarios: First, in the left plot of Fig. 6 $|V_{ub}|$ is determined such that the SM prediction of $\mathcal{B}(B \rightarrow \tau \nu)$ is equal to the experimental value. Using $f_B = (191 \pm 13) \text{ MeV}$ one gets $|V_{ub}| = (5.04 \pm 0.64) \cdot 10^{-3}$ [34]. In the plot we set $\mathcal{B}(B \rightarrow \tau \nu)^{\text{SM}} = \mathcal{B}(B \rightarrow \tau \nu)^{\text{exp}}$ and use the experimental 3σ -region. Second, in the right plot of Fig. 6 V_{ub} is fixed to the best-fit value of a global fit to the unitarity triangle [38]. An essential assumption of the second scenario is the absence of new physics in the CP asymmetry $A_{\text{CP}}^{\text{mix}}(B \rightarrow J/\psi K_S)$, from which the angle β of the unitarity triangle is determined: Then $|V_{ub}| \propto |V_{cb}| \frac{\sin \beta}{\sin \alpha}$ leads to $|V_{ub}| = (3.41 \pm 0.15) \cdot 10^{-3}$ [34]. In this case the SM central value $\mathcal{B}(B \rightarrow \tau \nu)^{\text{SM}} = 0.75 \cdot 10^{-4}$ is much lower than the experimental value and the SUSY contribution makes it even smaller. Therefore now $\mathcal{B}(B \rightarrow \tau \nu)$ is much more constraining than in the scenario of the left plot. Using the 2σ region of the experimental value one would exclude the whole $(M_{H^\pm}, \tan \beta)$ region (except for a very narrow strip with $\tan \beta \approx 0.3 M_{H^+}$); the constraint from the 3σ region is shown in the right plot of Fig. 6. In the future also $\mathcal{B}(B \rightarrow D \tau \nu)$ [37, 39, 40] and $\mathcal{B}(B \rightarrow \pi \tau \nu)$ [41] will probe charged-Higgs effects and will eventually shed light on the situation.

We finally mention two related studies: A prospective error of 0.12% of the NA62 experiment at CERN is used in Ref. [42]. The parameter scan in this paper respects $|\delta_{LL}^{13} \delta_{RR}^{13}| \leq 0.01$, in agreement with our result. In Ref. [43] it is pointed out, using a general effective theory approach, that in models with Minimal Lepton Flavour Violation (MLFV and MFV-GUT) the effects are too small to be observed.

4 Conclusions

The NA62 experiment has the potential to discover new sources of lepton flavour violation by testing lepton flavour universality through a precision measurement of $R_K = \Gamma(K \rightarrow e \nu) / \Gamma(K \rightarrow \mu \nu)$ [8].

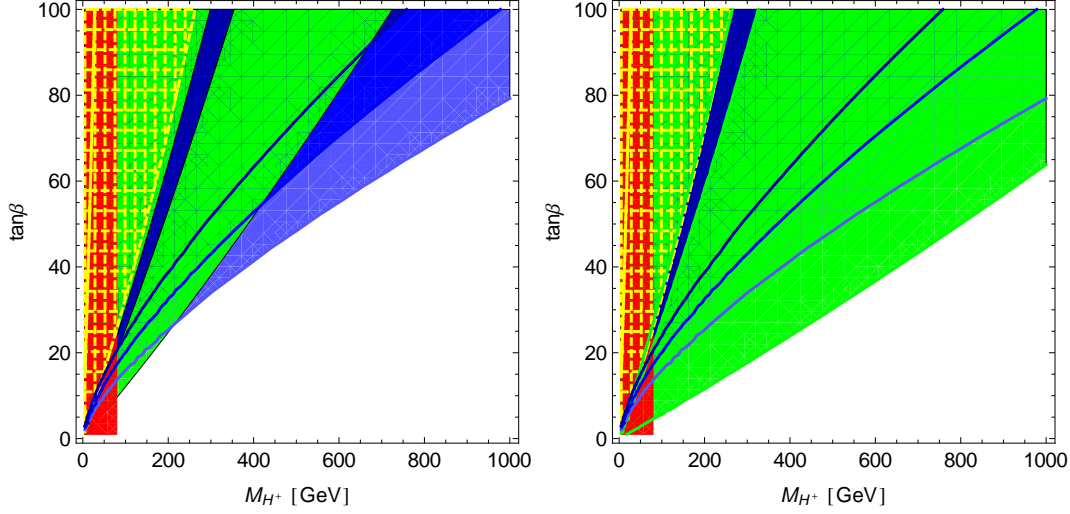


Figure 6: Regions with $\Delta r^{\mu-e} \geq 0.5\%$ for $\delta_{RR}^{13} = 0.15$ (darkblue), 0.25 (blue and darkblue), 0.5 (lightblue, blue, and darkblue). Overlaid in red: excluded by LEP H^+ searches; yellow dashed: 3σ exclusion limit from $R_{\mu 23}$; green: 3σ exclusion limit from $B \rightarrow \tau\nu$ (left: using $|V_{ub}| = (5.04 \pm 0.64) \cdot 10^{-3}$; right: using $|V_{ub}| = (3.41 \pm 0.15) \cdot 10^{-3}$).

This kind of new physics dominantly affects the decay rate $\Gamma(K \rightarrow e\nu)$. A lepton-flavour conserving (LFC) mechanism changing $\Gamma(K \rightarrow e\nu_e)$ may suppress or enhance R_K , while new lepton-flavour violating (LFV) decay modes such as $\Gamma(K \rightarrow e\nu_\tau)$ can only enhance R_K over its SM value. In this paper we have studied $\Delta r^{\mu-e} \equiv R_K/R_K^{\text{SM}} - 1$ in the MSSM, extending the analyses of Refs. [8, 27].

The LFC contribution to $\Delta r^{\mu-e}$ is driven by the parameter combination $\delta_{LL}^{13}\delta_{RR}^{13}$. In Ref. [12] it has been found that upper bounds on $|\delta_{LL}^{13}\delta_{RR}^{13}|$ can be derived from naturalness considerations of the electron mass and from the precise measurement of the anomalous magnetic moment of the electron. (Coincidentally, these two quantities give very similar constraints.) In Sect. 2 we have found that these bounds imply $|\Delta r_{\text{LFC}}^{\mu-e}| \lesssim 0.005$ and thereby challenge the large values for $|\Delta r_{\text{LFC}}^{\mu-e}|$ considered in Ref. [8]. At the same time our result is fully compatible with the range for $\Delta r_{\text{LFC}}^{\mu-e}$ advocated in Ref. [27]. The naturalness bound extends beyond the MSSM to a larger class of models, namely those with the tree-level Higgs sector of a 2HDM of type II.

The LFV contribution to $\Delta r^{\mu-e}$ can be larger, because a non-zero parameter δ_{RR}^{13} suffices to open the decay channel $K \rightarrow e\nu_\tau$ and δ_{RR}^{13} is only poorly constrained from other processes. We have calculated $\Delta r_{\text{LFV}}^{\mu-e}$ in Sect. 3 and found that the proper inclusion of $\tilde{\tau}_L$ - $\tilde{\tau}_R$ mixing is essential. The analytical expressions in Refs. [8, 27] include the $\tilde{\tau}_L$ - $\tilde{\tau}_R$ flip using the mass insertion approximation instead of the exact diagonalisation of the stau mass matrix. The interesting region of parameter space probed by NA62 corresponds to large values of μ and a sizable stau mixing angle θ_τ and in this region the left (bino) diagram in Fig. 2 is dominant. The formulae derived by us are also valid beyond the decoupling limit $M_{\text{SUSY}} \rightarrow \infty$, in which θ_τ vanishes. In order to facilitate the combination of future NA62 results with limits or measurements from high- p_T experiments, we have expressed $\Delta r_{\text{LFV}}^{\mu-e}$ in terms of the mass $m_{\tilde{\tau}_1}$ of the lightest stau eigenstate and the mixing angle θ_τ . For example, for $\tan\beta = 50$, $\mu = 800$ GeV, $\delta_{RR}^{13} = 0.5$, a charged-Higgs mass of $M_H = 500$ GeV, $m_{\tilde{\tau}_1} = 120$ GeV, a bino mass of $M_1 = 100$ GeV and a right-handed selectron mass of $m_{\tilde{e}_R} = 200$ GeV we find a maximal value of $\Delta r_{\text{LFV}}^{\mu-e} = 0.006$ corresponding to $\theta_\tau = 26^\circ$. In Eq. (30) we have derived an easy-

to-use formula expressing $\Delta r_{\text{LFV}}^{\mu-e}$ in terms of the relevant MSSM parameters. Finally we have plotted the regions of the MSSM parameter space probed by R_K and briefly compared the result with the constraint from other observables such as $\mathcal{B}(B \rightarrow \tau\nu)$.

Acknowledgements

The presented work is supported by BMBF Grant No.05H09VKF. J.G. acknowledges the financial support by *Studienstiftung des deutschen Volkes* and the DFG cluster of excellence “Origin and Structure of the Universe”. U.N. is grateful for the hospitality of the *Institute for Advanced Study* of Technische Universität München, where this paper has been completed.

References

- [1] B. Pontecorvo, *Inverse beta processes and nonconservation of lepton charge*, *Sov. Phys. JETP* **7** (1958) 172–173.
- [2] Z. Maki, M. Nakagawa, and S. Sakata, *Remarks on the unified model of elementary particles*, *Prog. Theor. Phys.* **28** (1962) 870–880.
- [3] P. Minkowski, $\mu \rightarrow e\gamma$ at a Rate of One Out of 1-Billion Muon Decays?, *Phys. Lett.* **B67** (1977) 421.
- [4] T. Yanagida, *Horizontal symmetry and masses of neutrinos*, *Conf.Proc.* **C7902131** (1979) 95.
- [5] S. Glashow, *The future of elementary particle physics*, *NATO Adv.Study Inst.Ser.B Phys.* **59** (1980) 687. Preliminary version given at Colloquium in Honor of A. Visconti, Marseille-Luminy Univ., Jul 1979.
- [6] M. Gell-Mann, P. Ramond, and R. Slansky, *Complex spinors and unified theories*, *Conf.Proc.* **C790927** (1979) 315–321. To be published in *Supergravity*, P. van Nieuwenhuizen and D.Z. Freedman (eds.), North Holland Publ. Co., 1979.
- [7] R. N. Mohapatra and G. Senjanovic, *Neutrino Mass and Spontaneous Parity Violation*, *Phys.Rev.Lett.* **44** (1980) 912.
- [8] A. Masiero, P. Paradisi, and R. Petronzio, *Probing new physics through $\mu - e$ universality in $K \rightarrow l\nu$* , *Phys. Rev.* **D74** (2006) 011701, [hep-ph/0511289].
- [9] M. Finkemeier, *Radiative corrections to π_{l2} and K_{l2} decays*, *Phys. Lett.* **B387** (1996) 391–394, [hep-ph/9505434].
- [10] V. Cirigliano and I. Rosell, *Two-loop effective theory analysis of $\pi K \rightarrow e\bar{\nu}_e(\gamma)$ branching ratios*, *Phys.Rev.Lett.* **99** (2007) 231801, [arXiv:0707.3439].
- [11] V. Cirigliano and I. Rosell, *$\pi/K \rightarrow e\nu$ branching ratios to $O(e^2p^4)$ in Chiral Perturbation Theory*, *JHEP* **10** (2007) 005, [0707.4464].
- [12] J. Girrbach, S. Mertens, U. Nierste, and S. Wiesenfeldt, *Lepton flavour violation in the MSSM*, *JHEP* **05** (2010) 026, [arXiv:0910.2663].

-
- [13] **Particle Data Group** Collaboration, K. Nakamura *et. al.*, *Review of particle physics*, *J. Phys.* **G37** (2010) 075021.
 - [14] G. Isidori, *KAON 2007: Conference Summary*, *PoS KAON* (2006) 064, [arXiv:0709.2438].
 - [15] **KLOE** Collaboration, F. Ambrosino *et. al.*, *Precise measurement of $B(K \rightarrow e\nu(\gamma))/B(K \rightarrow \mu\nu(\gamma))$ and study of $K \rightarrow e\nu\gamma$* , *Eur.Phys.J.* **C64** (2009) 627–636, [arXiv:0907.3594].
 - [16] **NA62** Collaboration, E. Goudzovski, *Lepton flavour universality test at the CERN NA62 experiment*, *Nucl.Phys.Proc.Suppl.* **210-211** (2011) 163–168, [arXiv:1008.1219].
 - [17] E. Goudzovski, *Talk at NA62 Physics Handbook Workshop, CERN* (2009).
 - [18] **NA62** Collaboration, C. Lazzeroni *et. al.*, *Test of Lepton Flavour Universality in $K^+ \rightarrow l^+\nu$ Decays*, *Phys.Lett.* **B698** (2011) 105–114, [arXiv:1101.4805].
 - [19] E. Goudzovski, *Lepton flavour and number violation with K decays at CERN, Talk at 46th Rencontres de Moriond, La Thuile, Italy* (2011).
 - [20] E. Goudzovski, *Kaon experiments at CERN: NA48 and NA62*, arXiv:1112.5365.
 - [21] **NA48/2 and NA62** Collaboration, E. Goudzovski, *Kaon programme at CERN: recent results*, arXiv:1111.2818.
 - [22] W.-S. Hou, *Enhanced charged Higgs boson effects in $B^- \rightarrow \tau\nu, \mu\nu$ and $b \rightarrow \tau\nu + X$* , *Phys. Rev.* **D48** (1993) 2342–2344.
 - [23] L. J. Hall, R. Rattazzi, and U. Sarid, *The Top quark mass in supersymmetric $SO(10)$ unification*, *Phys. Rev.* **D50** (1994) 7048–7065, [hep-ph/9306309].
 - [24] M. S. Carena, D. Garcia, U. Nierste, and C. E. M. Wagner, *Effective Lagrangian for the $\bar{t}bH^+$ interaction in the MSSM and charged Higgs phenomenology*, *Nucl. Phys.* **B577** (2000) 88–120, [hep-ph/9912516].
 - [25] L. Hofer, U. Nierste, and D. Scherer, *Resummation of $\tan\beta$ -enhanced supersymmetric loop corrections beyond the decoupling limit*, *JHEP* **0910** (2009) 081, [arXiv:0907.5408].
 - [26] S. Marchetti, S. Mertens, U. Nierste, and D. Stockinger, *$\tan\beta$ -enhanced supersymmetric corrections to the anomalous magnetic moment of the muon*, *Phys. Rev.* **D79** (2009) 013010, [arXiv:0808.1530].
 - [27] A. Masiero, P. Paradisi, and R. Petronzio, *Anatomy and Phenomenology of the Lepton Flavor Universality in SUSY Theories*, *JHEP* **11** (2008) 042, [arXiv:0807.4721].
 - [28] A. Crivellin and J. Girrbach, *Constraining the MSSM sfermion mass matrices with light fermion masses*, *Phys. Rev.* **D81** (2010) 076001, [arXiv:1002.0227].
 - [29] J. Hisano, M. Nagai, and P. Paradisi, *Flavor effects on the electric dipole moments in supersymmetric theories: A beyond leading order analysis*, *Phys.Rev.* **D80** (2009) 095014, [arXiv:0812.4283].

-
- [30] A. J. Buras, P. H. Chankowski, J. Rosiek, and L. Slawianowska, $\Delta M_{d,s}$, $B_{d,s}^0 \rightarrow \mu^+ \mu^-$ and $B \rightarrow X_s \gamma$ in supersymmetry at large $\tan \beta$, *Nucl. Phys.* **B659** (2003) 3, [hep-ph/0210145].
 - [31] J. Hisano, M. Nagai, P. Paradisi, and Y. Shimizu, *Waiting for $\mu \rightarrow e \gamma$ from the MEG experiment*, *JHEP* **0912** (2009) 030, [arXiv:0904.2080].
 - [32] P. Paradisi, *Higgs-mediated $e \rightarrow \mu$ transitions in II Higgs doublet model and supersymmetry*, *JHEP* **08** (2006) 047, [hep-ph/0601100].
 - [33] M. Antonelli, V. Cirigliano, G. Isidori, F. Mescia, M. Moulson, *et. al.*, *An Evaluation of $|V_{us}|$ and precise tests of the Standard Model from world data on leptonic and semileptonic kaon decays*, *Eur.Phys.J.* **C69** (2010) 399–424, [arXiv:1005.2323].
 - [34] U. Nierste, *Flavour Physics, supersymmetry and GUTs, talk at The Role of Heavy Fermions in Fundamental Physics, April 11-14, Portorož, Slovenia* (2011).
 - [35] U. Nierste, *Flavour physics, supersymmetry and grand unification, talk at 46th Rencontres de Moriond on Electroweak Interactions and unified Theories, 13-20 Mar 2011, La Thuile, Italy* (2011) [arXiv:1107.0621].
 - [36] **BABAR** Collaboration, R. Barlow, *Experimental status of $B \rightarrow \tau \nu$ and $B \rightarrow \ell \nu(\gamma)$* , arXiv:1102.1267.
 - [37] U. Nierste, S. Trine, and S. Westhoff, *Charged-Higgs effects in a new $B \rightarrow D \tau \nu$ differential decay distribution*, *Phys.Rev.* **D78** (2008) 015006, [arXiv:0801.4938].
 - [38] A. Lenz, U. Nierste, J. Charles, S. Descotes-Genon, A. Jantsch, *et. al.*, *Anatomy of New Physics in $B - \bar{B}$ mixing*, *Phys.Rev.* **D83** (2011) 036004, [arXiv:1008.1593].
 - [39] J. F. Kamenik and F. Mescia, *$B \rightarrow D \tau \nu$ Branching Ratios: Opportunity for Lattice QCD and Hadron Colliders*, *Phys.Rev.* **D78** (2008) 014003, [arXiv:0802.3790].
 - [40] M. Tanaka and R. Watanabe, *Tau longitudinal polarization in $B \rightarrow D \tau \nu$ and its role in the search for charged Higgs boson*, *Phys.Rev.* **D82** (2010) 034027, [arXiv:1005.4306].
 - [41] A. Khodjamirian, T. Mannel, N. Offen, and Y.-M. Wang, *$B \rightarrow \pi \ell \nu_l$ Width and $|V_{ub}|$ from QCD Light-Cone Sum Rules*, *Phys.Rev.* **D83** (2011) 094031, [arXiv:1103.2655].
 - [42] J. Ellis, S. Lola, and M. Raidal, *Supersymmetric Grand Unification and Lepton Universality in $K \rightarrow l \nu$ Decays*, *Nucl.Phys.* **B812** (2009) 128–143, [arXiv:0809.5211].
 - [43] A. Filipuzzi and G. Isidori, *Violations of lepton-flavour universality in $P \rightarrow l \nu$ decays: a model-independent analysis*, *Eur.Phys.J.* **C64** (2009) 55–62, [arXiv:0906.3024].